Nucleation and Propagation of Cracks in Polystyrene

J. MURRAY and D. HULL

Tensile tests have been made on compression moulded polystyrene at 293°K to determine the processes associated with the nucleation and propagation of cracks. Optical and electron microscope replica techniques have been used to study the microscopic details of the deformation mechanisms prior to fracture and the characteristics of the fracture surface. It is shown that fracture is preceded by the formation of crazes and that at a critical stage small voids form in the thickest part of the craze. The voids coalesce and form a planar cavity which then propagates within the craze gradually increasing in velocity. A number of stages in the fracture process are identified and the importance of the initial structure of the moulded material is emphasized.

RECENT studies[1] of the fracture of glassy amorphous plastics have shown that there is close connection between crazing and the nucleation and propagation of cracks. In particular, Mann[2] has shown conclusively that in injection moulded polystyrene specimens the cracks formed in close association with a preformed craze. Similarly, Kambour[3] using wedging type experiments to study the slow propagation of cracks, introduced artificially, has shown that a zone of crazed material forms ahead of the crack. It follows that a detailed knowledge of the properties of crazes and the relation between crazing and fracture is required for a full understanding of the fracture process.

EXPERIMENTAL DETAILS

Large sheets approximately 0·3 cm thick of polystyrene were produced by compression moulding Carinex G.P. The material was preheated at temperatures between 430° and 460°K for 15 minutes and then compressed at

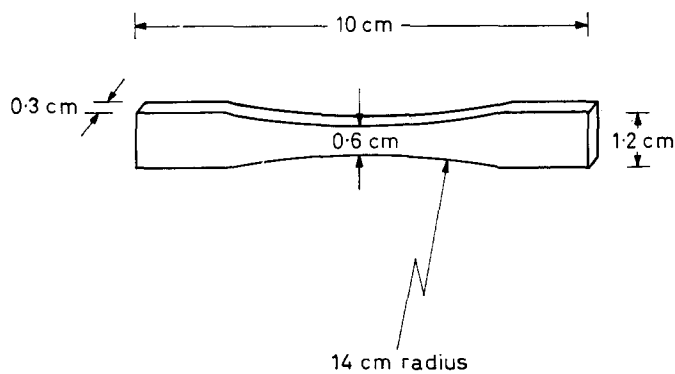

Figure 1—Shape and dimensions of tensile specimens

pressures between 0·35 and 1·06 kg mm^{-2} for a further 15 minutes. After moulding, some sheets were air cooled, between backing plates, from the moulding temperature and others were quenched into water.

Tensile specimens were cut from the sheet using a jewellers' saw. The dimensions of the specimen are given in *Figure 1*. The most important feature is the large radius of curvature formed along the gauge length to minimize stress concentrations. The edges of the specimen were hand ground on emery papers down to grade 4/0 and then polished with 'Gamma' Alumina paste (the finest grade available, particle size not known but less than 1·5 microns).

The tensile tests were carried out in an Instron tensile machine with a crosshead speed of 0·05 cm min^{-1}. The majority of the tests were at ambient temperatures in atmosphere. A few tests were made at 195°K by surrounding the specimens with crushed Cardice.

The changes in surface structure during tensile tests were followed with optical microscopy and the appearance of deformed and fractured specimens was studied using optical and electron microscopy. The optical microscopy included interferometric studies and these are described in the results section where appropriate. Electron microscopy was confined to examination of fracture surfaces. The surface of the fracture was shadowed at 20° to the surface with a gold–palladium alloy. This was then backed with a vapour deposited carbon layer which was separated from the plastic using carbon tetrachloride as a solvent.

EXPERIMENTAL OBSERVATIONS

(i) *General features*

At 293°K the tensile specimens fractured in a brittle manner after a crosshead displacement of about 0·095 cm. The shape of the specimen used precludes a precise description of the relation between stress and strain. However, the typical load/displacement plot shown in *Figure 2* indicates

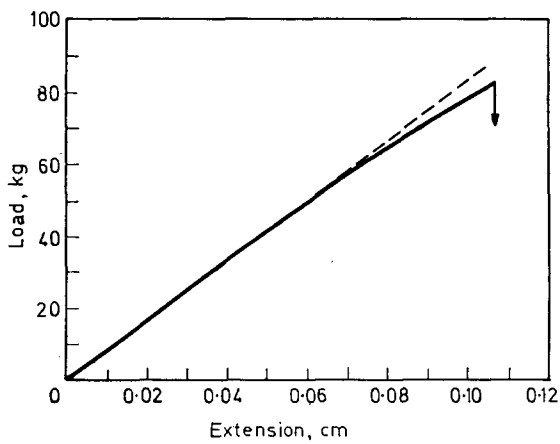

Figure 2—Load/extension curve for tensile specimens deformed at 293°K

that the deviation from linear behaviour occurs at about half the final fracture stress and that the actual deviation is small. The fracture stress, calculated from the load at fracture and the cross-sectional area at fracture, was $4{\cdot}05 \pm 0{\cdot}02$ kg mm^{-2}. There was no obvious correlation between fracture behaviour and moulding history and within the context of the present observations the latter is considered to be unimportant.

Direct observation of the specimen during tensile extension revealed that at about 40 per cent of the fracture load very fine craze markings formed normal to the tensile axis in the centre of the gauge length. The highest density of markings was approximately 50 to 100 mm^{-2} at the surface. As the load increased the crazes became more prominent and increased in length. New craze markings also formed. The majority of the fine crazes formed at the surface and it was generally possible to detect a small dark speck in each craze. This is in agreement with the observations of Wolock, Kies and Newman[4] which indicated that the crazes were nucleated by fine particles. The source of these particles is not known. At loads between 85 and 90 per cent of the fracture load a small number of much larger crazes developed. These formed at the surface and in the interior of the specimens and were readily detected with the naked eye. The large crazes spread rapidly across the specimen normal to the tensile axis and eventually fracture occurred by crack formation and propagation within one of these large crazes.

The fracture surface can be divided into a number of different areas with characteristic features which were entirely consistent from one specimen to the next. In particular, it was possible to identify the source of fracture and follow the changes in the fracture surface as the crack propagated. These features are described in the next section but one. To determine the sequence of events immediately before fracture the structure of the large crazes was studied by sectioning the specimen to produce thin slices parallel to the crazes. These observations are described in the next section.

(ii) *Geometry of uncracked crazes*

The shape of the slices cut from unfractured specimens is illustrated in *Figure 3* which also shows the position of the craze parallel to the plane of the

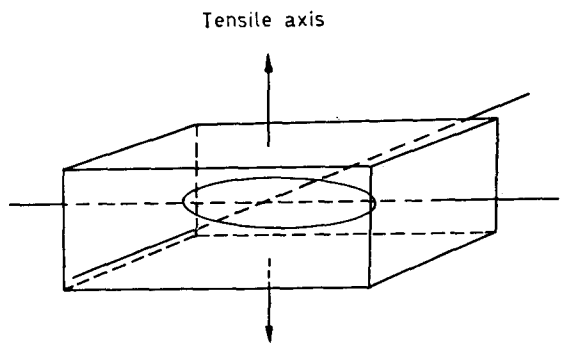

Figure 3—Shape of specimens cut from tensile specimens to examine shape of crazes in unfractured specimens

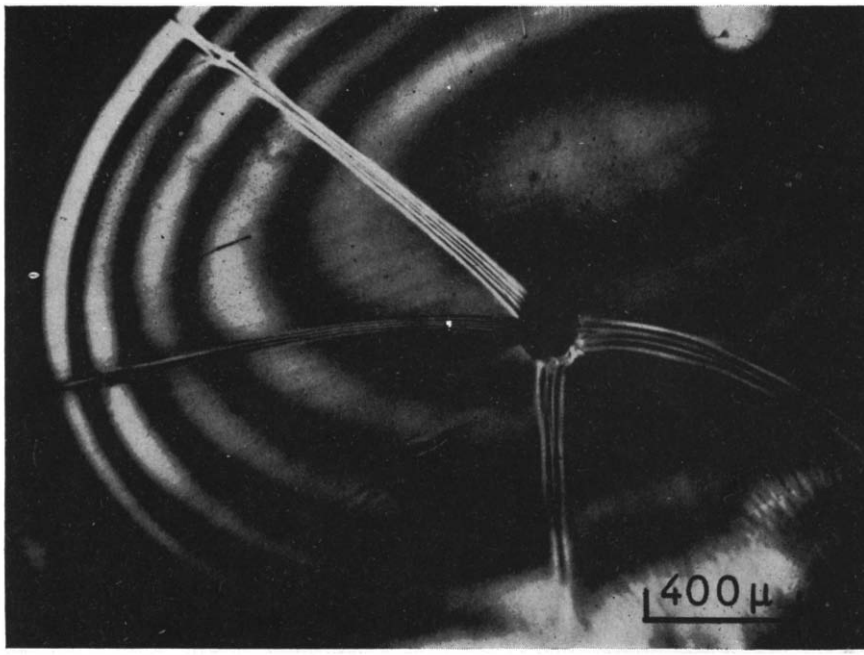

Figure 4—Reflected light micrograph of an internal craze

slice and normal to the direction of observation and the original tensile axis. In the optical microscope the crazes are revealed as a series of concentric interference fringes, *Figure 4*. Following Kambour, the fringe pattern can be interpreted as resulting from interference between light reflected from the top and bottom surfaces of the craze, which has a refractive index $\mu_c < \mu_m$, the refractive index of the matrix. The thickness of the craze was determined from the position of the fringes using monochromatic light ($\lambda = 6\,000$Å) and assuming $\mu_c = 1{\cdot}33$ which is the value determined by Kambour for craze

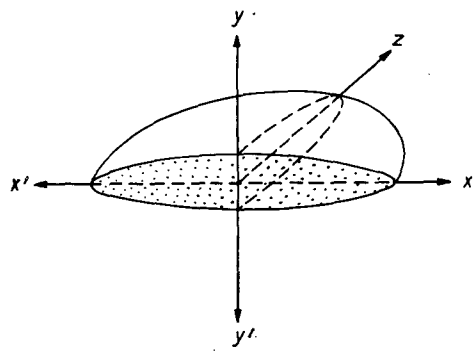

Figure 5—Diagrammatic representation of the shape of a craze

material in unstressed polystyrene[5]. The general three-dimensional shape of the craze is illustrated schematically in *Figure 5*, and in *Figure 6* the dimensions of the crazes for the sections shown in *Figure 5* are represented graphically for two typical crazes. It has been assumed that the shape of the craze is symmetrical about the plane $y=0$, although this information cannot be obtained from the interference fringes. The large craze illustrated in *Figure 6* is elliptical in the plane of the craze, cf. *Figure 4*, whereas the smaller craze in *Figure 6* is approximately circular.

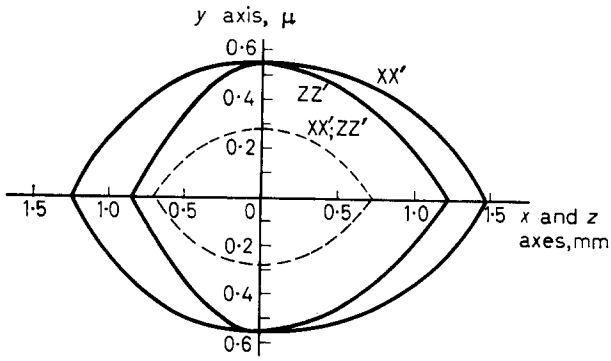

Figure 6—Dimensions of two typical crazes shown as sections parallel to *xy* and *zy* planes (see *Figure 5*)

All the crazes studied contained a number of internal features. Close to the centre of even the smallest internal craze there was an irregular particle or spherical bubble, cf. *Figure 4*. In many of the crazes spike-like features radiated outwards from the particle or bubble as shown in *Figure 4*. These spikes were visible because of an optical interference effect but it has not been possible to identify conclusively the cause or character of the spikes. There is evidence that they are produced at the overlap between planar regions of craze which lie at slightly different levels. The most important features, observed primarily in the larger crazes, were elongated finger-like cavities which we have called 'events'. These events formed in the thicker parts of the craze and were not normally associated with the irregular particles or bubbles mentioned above. A typical event is shown in *Figure 7*. Some events consist of a single finger region and others are made up of two or more such fingers spreading out from a junction. The events were often aligned parallel to the long dimensions of the specimen cross section. In white light the events appeared as single coloured regions surrounded by the coloured fringe pattern of the craze. Similarly in monochromatic light the events were free from a fringe structure, indicating that the faces of the event were parallel sided. Evidence that the events are cavities is presented in the next section.

In the course of some preliminary experiments on the growth of crazes at low temperatures, specimens containing crazes and events formed at 293°K were subsequently subjected to tensile loading at 195°K. The application of stress resulted in the appearance of a fine substructure. The crazes

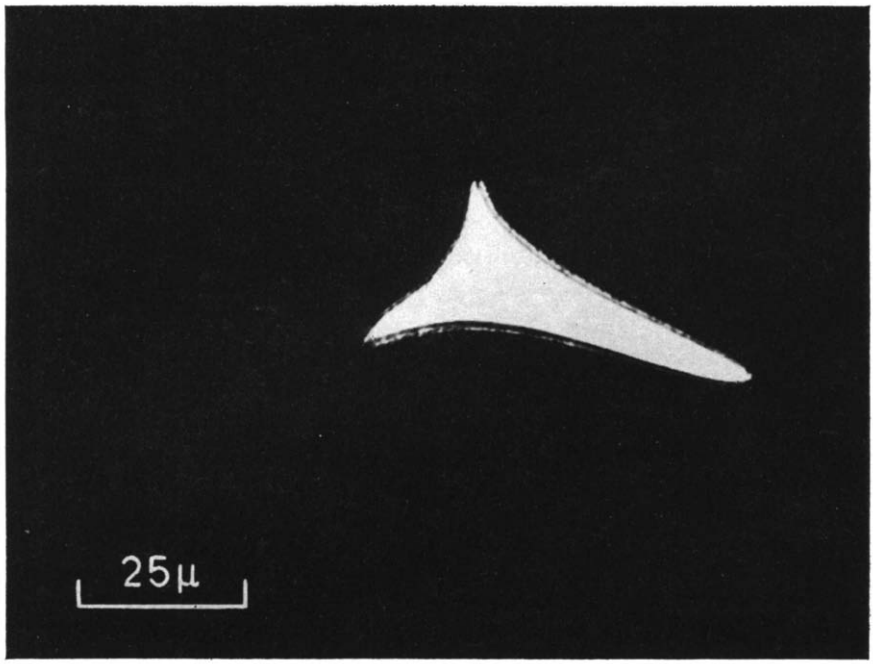

Figure 7—Reflected light micrograph of a planar cavity inside an internal craze

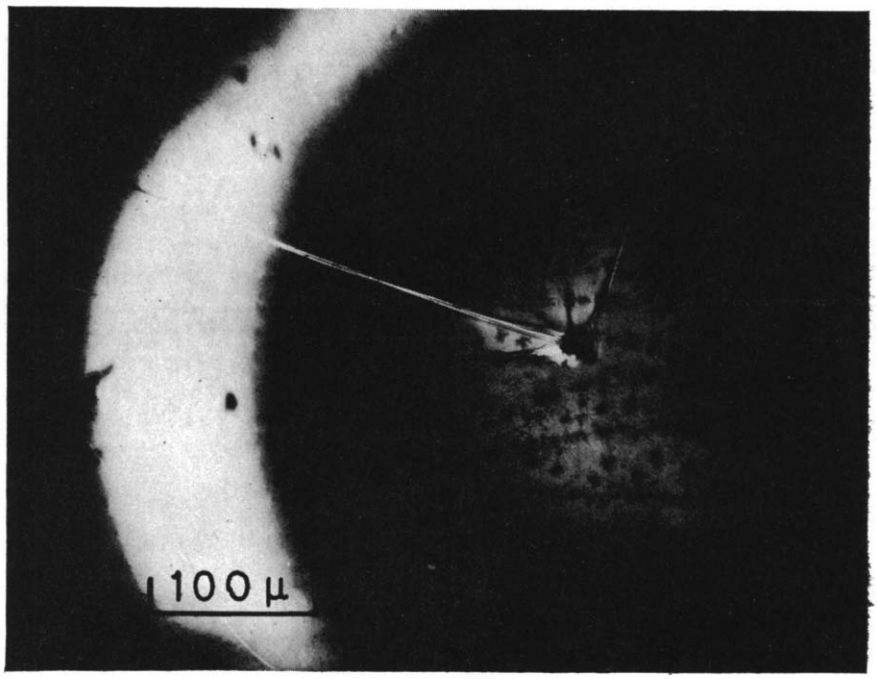

Figure 8—Reflected light micrograph showing the substructure pattern inside an internal craze which was formed at 293°K and subsequently stressed at 195°K

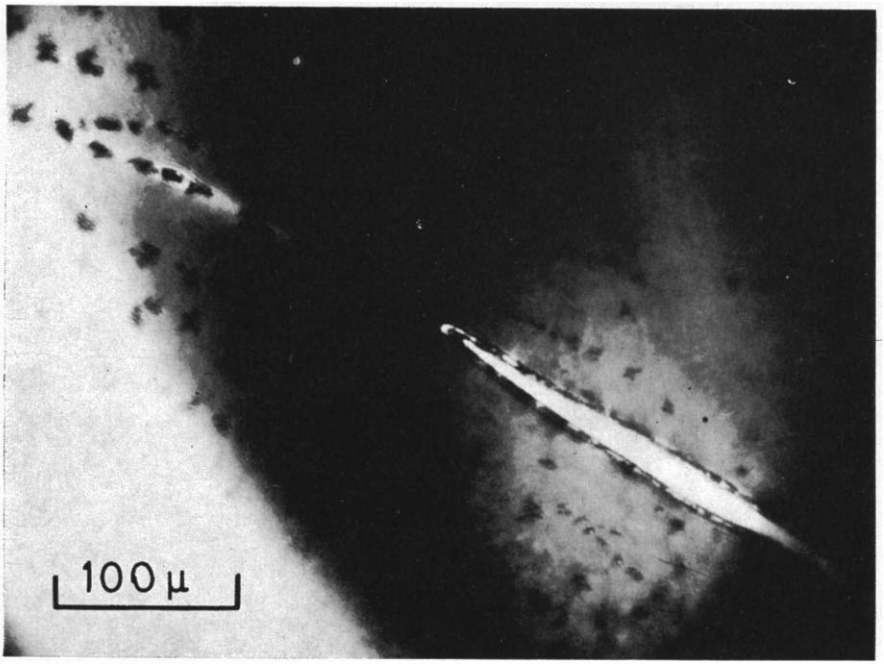

Figure 9—Reflected light micrograph of a planar cavity which has formed along a substructure boundary. Specimen tested at 293°K and restressed at 195°K

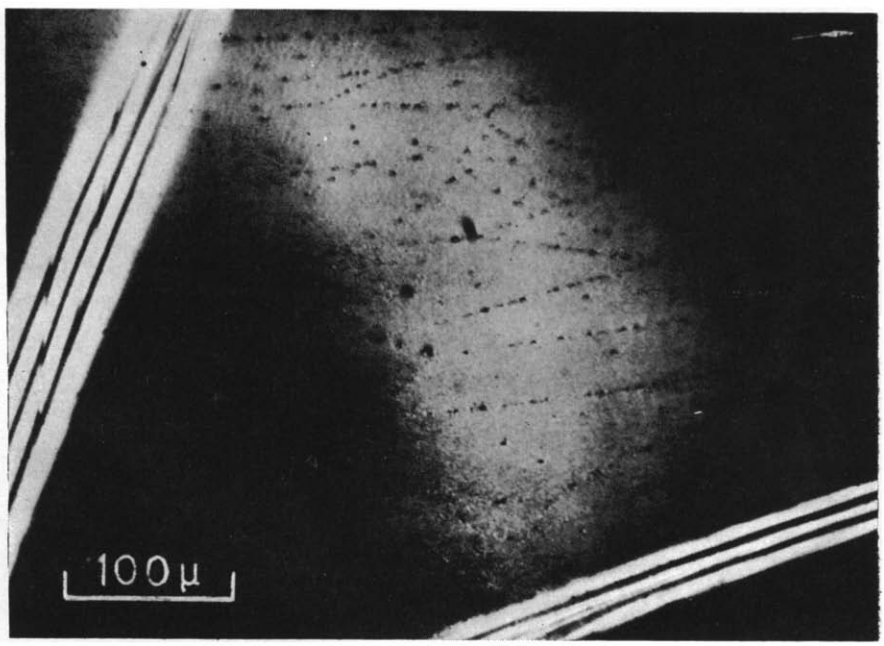

Figure 10—Reflected light micrograph of part of an internal craze formed at 293°K after it had been stressed at 195°K and annealed at 340°K. Note: the star-shaped regions in *Figures 8* and *9* have disappeared leaving tiny particles and cavities

were divided up into elongated areas by sub-boundaries made up of small star-shaped regions, as shown in *Figure 8*. There was a close correlation between events formed at 293°K and the star-shaped regions as illustrated in *Figure 9*, indicating that the formation of the events is in some way related to the sub-boundary structure.

When crazes containing star-shaped regions were annealed at successively higher temperatures the star shapes gradually disappeared leaving behind small voids or particles, *Figure 10*. After heating to 363°K all traces of the craze had disappeared but the voids and events were still visible. The remaining events developed a fringe pattern indicating that their shape changed from a flat planar section to a more rounded form.

(iii) *Fracture surface studies*

It should be noted that the general features of polystyrene fracture surfaces have been studied by Bird *et al.*[6] using electron microscopy. The main features observed by these authors were confirmed in the present investigation and additional information obtained.

Surface studies were confined mainly to the 'mirror' area of fracture. Specimens tested under identical conditions exhibited similar fracture surfaces which could be divided up into several characteristic regions as illustrated schematically in *Figure 11*. An example of a fracture surface is shown in *Figure 12*. In the central region A the surface was covered with a

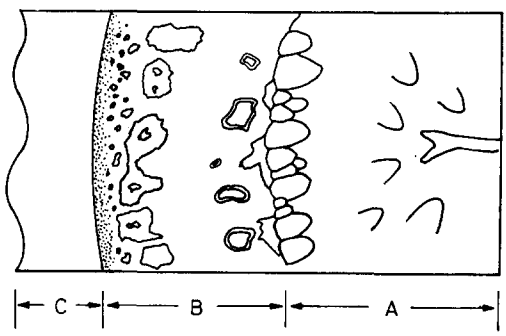

Figure 11—Diagram showing the different regions of the fracture surface typical of specimens tested in tension

fine texture of striations scattered with parabolic regions which have been ascribed [1, 7, 8] to sites of secondary fracture. From the direction of the striations and the position of the parabolas it is possible to trace back to the origin of the fracture. In every specimen examined the origin consisted of a region identical in form and shape to the 'events' described in the previous section. An example of the fracture origin is shown in *Figure 13*, and an electron micrograph of a small section of the event is shown in *Figure 14*. In the optical microscope the fracture surface is covered with interference fringes arising from the reflection of light from the fracture surface and the

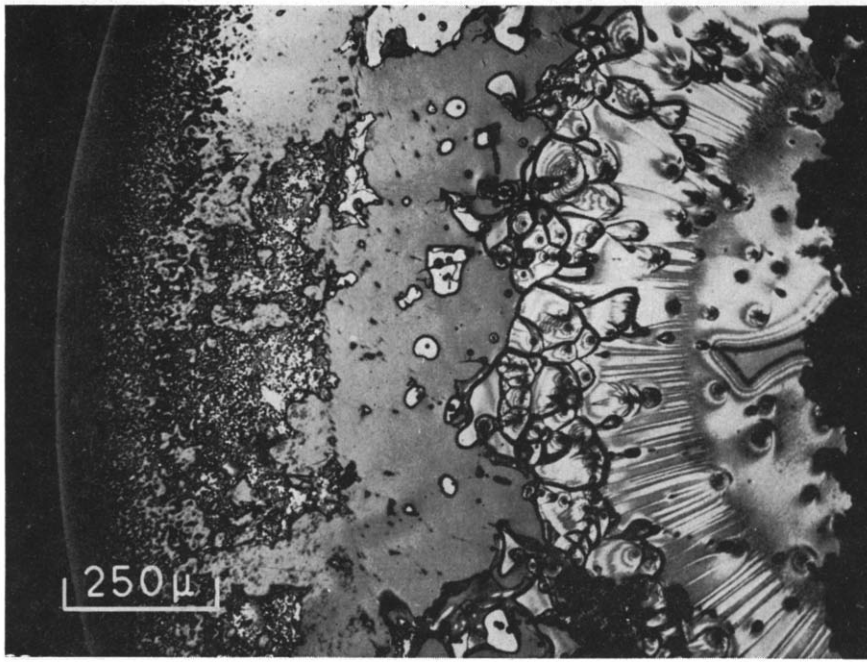

Figure 12—Optical fractograph of the mirror area on a specimen tested at 295°K

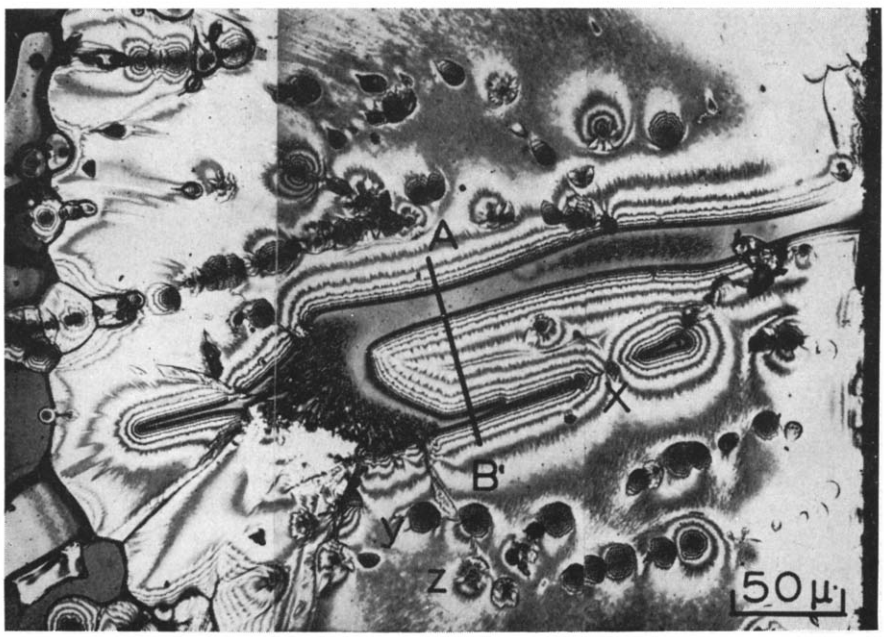

Figure 13—Optical fractrograph of the initiation stage of fracture showing the characteristic finger-shaped nucleation event and parabolas associated with secondary fractures

interface between the craze and undeformed material. The morphology of the craze at the surface can be found, therefore, from the interference patterns. Around the event the fringes consist of closely spaced parallel lines and in cross section this corresponds to a sharp step at the event boundary. The section A–B through the event in *Figure 13* is shown in *Figure 15*. The corresponding section on the other fracture face is also shown in *Figure 15* indicating that the steps are in the same sense on the two faces so that the event must correspond to a cavity. In this example the total displacement across the cavity is 3·2 microns. The depth of the cavity in fractured specimens was the same to within $\pm$ 0·1 micron in all room temperature specimens for a fixed crosshead speed. The striations in the

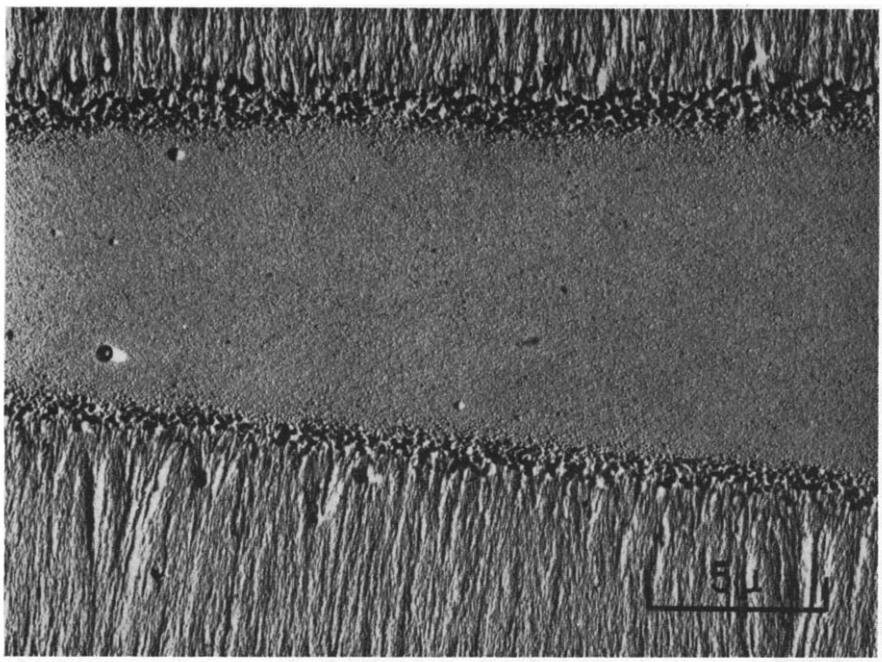

Figure 14—Electron micrograph of a shadowed carbon replica showing part of the 'event' region of the fracture surface

fracture surface spread out approximately normal to the edges of the event. In the optical microscope the bottom of the event is smooth apart from a rumpled surface which sometimes appears in the centre of the cavity (*Figure 13*). This rumpled surface appeared on both fracture surfaces. In the electron microscope (*Figure 14*) the bottom of the cavity has a fine granular structure. At the boundary between the cavity and the striations there is a coarse granular structure.

The parabolic regions were well defined and were of two kinds, namely, small depressions and hillocks on the generally planar fracture surface, see y and z on *Figure 13*. The shapes of these regions could be determined from the interference patterns and it was found that depressions on one fracture

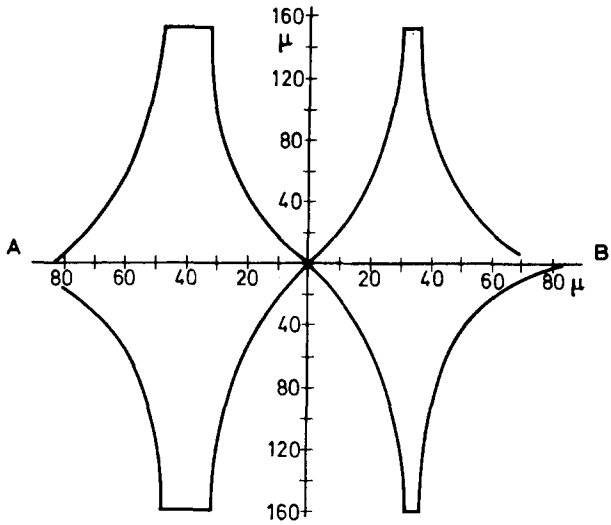

Figure 15—Dimensions of cross section A–B in *Figure 13*. The upper half of the diagram was measured on one fracture surface and the lower half from the other fracture surface. Note: both displacement scales are in microns

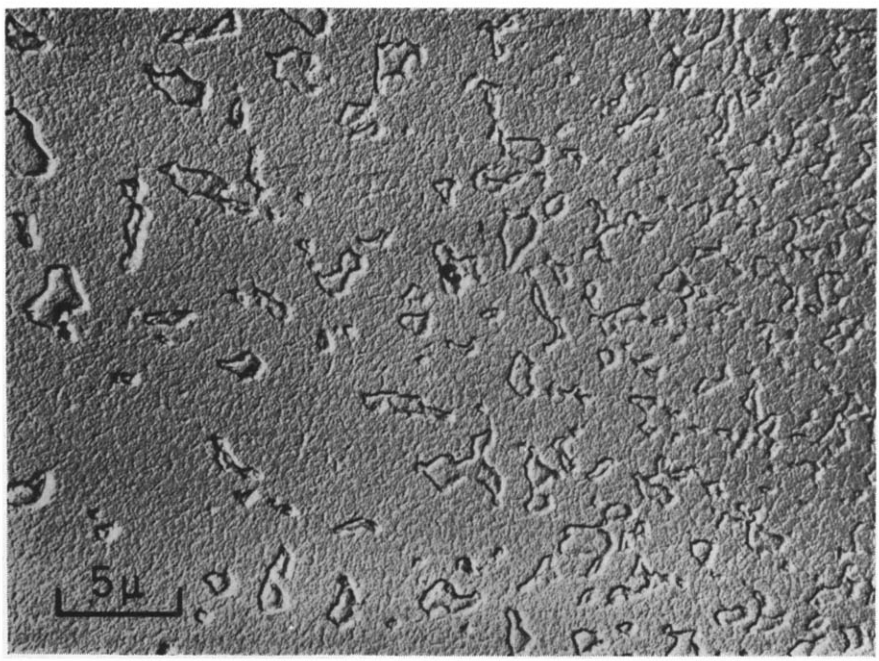

Figure 16—Electron micrograph of a shadowed carbon replica from the outer part of region B in *Figure 11*

surface corresponded to hillocks on the opposite fracture surface. This was confirmed by focusing at the top and bottom of the hillocks and depressions, using an objective with a very short depth of focus. It was not possible to confirm a perfect mating of the depression and hillock. Profile measurements and replica electron microscopy suggested that the depressions had a rounded bottom whereas the hillocks appeared to be topped by a crater with raised edges. The depth of all the depressions in a small area was approximately the same, and close to the events was approximately the same as the depth of the event. The distribution of parabolas was not random and was characterized by two separate factors. First, the density increased away from the initiating event and at the boundary of the region A they were closely spaced and overlapping. Secondly, in regions away from the boundary of region A the parabolas were often arranged in rows the general distribution of which closely resembled the sub-boundaries illustrated in *Figures 8* to *10*. It is also clear from *Figure 13* that the general path of the event follows the same pattern and at point X the event has propagated between two particles in one of the rows. Biplanar regions, as observed by Berry[8] in PMMA, were observed in most specimens on the fracture surface.

The main feature of the fracture surface in region B, outside the band of closely spaced parabolas, was the occurrence of thin sheets of polymer which adhered to one or other of the two fracture faces. The surfaces not covered by the sheet appeared to be very smooth even in the electron microscope (*Figure 16*). In the optical microscope the sheet showed many interference

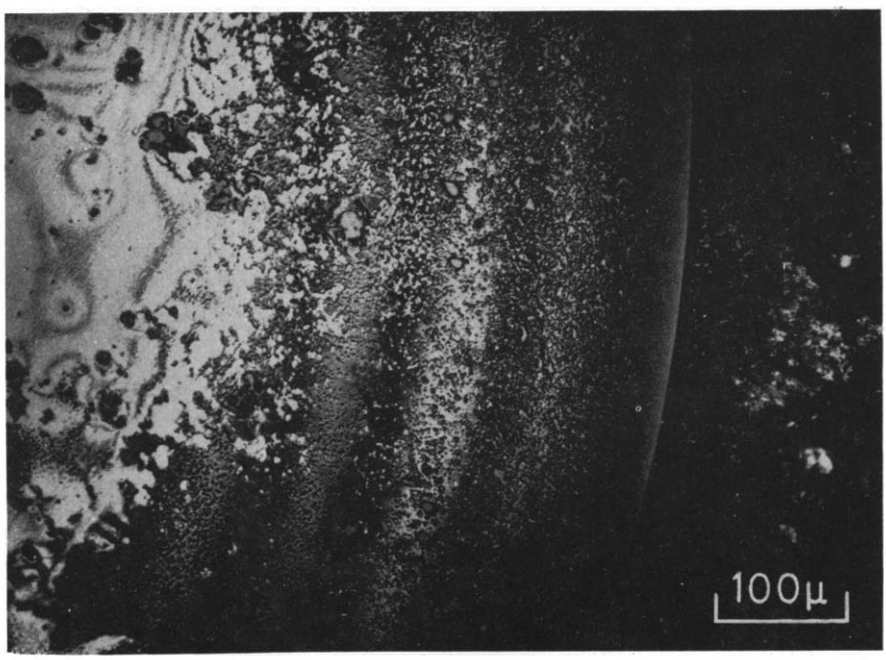

Figure 17—Optical fractograph showing the transition from region B to region C in *Figure 11*

patterns characteristic of craze material. Immediately outside region A the sheets extended over large areas of the fracture surface. At larger distances from the fracture source the size of the sheets became progressively finer until they were barely resolvable in the optical microscope (*Figure 17*). The larger sheets appeared to be only loosely held to the main body of the material and pieces of sheet were often seen with drawn whiskers on the outside edges of the individual sheets. In *Figure 17* broad interference fringes similar to those observed in crazes in unfractured specimens can be seen at the outside of region B.

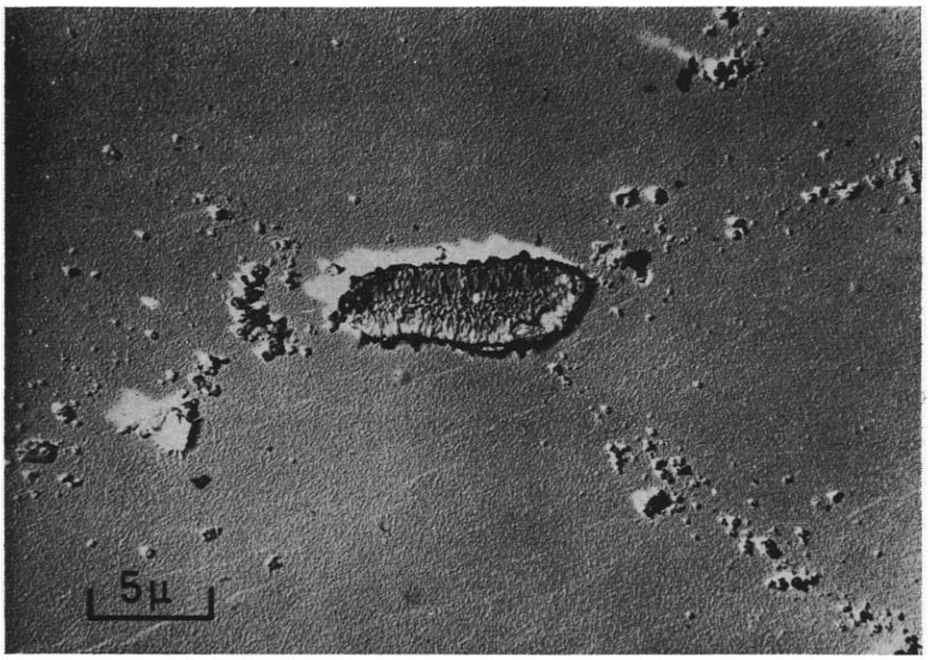

Figure 18—Electron micrograph of shadowed carbon replica showing fine particles lying along well defined boundaries and an embryo 'event'

On the fracture surface not covered by a film of craze a network of rows of inhomogeneities, consisting of irregular and spherical particles, was observed using replicas in the electron microscope (*Figure 18*). Selected area electron diffraction on particles extracted on the replicas showed them to be non-crystalline. The networks were distributed in the same way as the sub-boundaries described above in connection with the early stages of the formation of events. An embryo event which has formed in association with these boundaries is also shown in *Figure 18*.

The boundary between region B and region C defines the extent of smooth fracture and is approximately circular in shape. In region C the fracture path is irregular, highly distorted and accompanied by crack branching. At high magnification small smooth areas were visible. On the outside of the specimen the fracture path followed fine surface crazes produced in the early stages of deformation.

DISCUSSION

Using the value of the fracture stress, elastic modulus and fracture surface energy obtained by Berry[9] for polystyrene at 298°K gives a value of the 'natural flaw size' calculated from the Griffith relation of about 0·11 cm. In other words to explain the observed fracture stress using the idea that this is determined by the presence of a pre-existing crack, it is necessary to postulate that such cracks are 0·11 cm long. With the methods of specimen preparation and observation used in the present work such pre-existing cracks should be readily detectable. Since cracks were not found in unstressed specimens it is concluded that fracture results from the nucleation of cracks caused by the application of a tensile stress. The observations made in this work indicate that fracture at 293°K is preceded by a number of well defined stages. These stages are mutually self-consistent and provide a model for fracture which can be used in future work to interpret the variations of fracture behaviour, with, for example, temperature, strain rate, loading conditions and constitution.

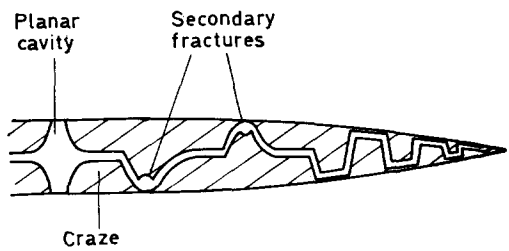

Figure 19—Diagrammatic representation of the sequence of events associated with the nucleation and propagation of fracture

The model which is illustrated schematically in *Figure 19* is as follows:

(a) Localized regions of plastic flow occur by the formation of fine crazes at microscopic or sub-microscopic inhomogeneities. The crazes grow as thin ellipsoidal regions with the principal plane of the ellipsoid normal to the applied tensile stress. These crazes form both at the surface of the material and internally.

(b) During the growth of the internal crazes and the thicker surface crazes small voids develop around inhomogeneities in the craze.

(c) The voids grow and coalesce to form a planar cavity within the craze, the thickness of the cavity being equal to the thickness of the craze. Evidence for void coalescence can be seen at point X in *Figure 13*.

(d) At a critical stage the planar void propagates as a crack by tearing of the craze material on a path parallel to, and in the centre of, the plane of the craze. The tearing crack interacts with cavities formed in other parts of the craze, some of which have coalesced to form planar voids, and produces secondary fracture surface features such as parabolas. The characteristic texture of the slow fracture surface has been attributed by Bird *et al.*[6] to

'lag and lead' of the moving crack front. This has been confirmed in the present work by the study of crack movement in cleavage-type experiments similar to those of Kambour[1].

(e) In the thinner regions of the craze the tearing-type fracture is followed by more rapid crack propagation which involves considerable local adiabatic heating as predicted by Kambour and Barker[10], and results in a highly drawn fibrous fracture surface.

(f) The crack propagates catastrophically on an irregular path due to, for example, nucleation of multiple cracks and crack branching as a result of the change in stress distribution around a rapidly moving crack (Yoffe[11].)

The distribution of cavities in the form of a three-dimensional network observed in this work suggests that the small inhomogeneities responsible are introduced either as a lubricant applied after polymerization or in the moulding process as fine dust. The average network size is comparable to the particle size of the initial Carinex stock material so that although the moulding temperature was sufficiently high above T_g to produce effective welding the inhomogeneities remained at the original boundaries. The process which leads to nucleation and growth of voids is undoubtedly dependent on the mobility of the polystyrene molecules but a detailed model of this process requires considerable experimental work before the important parameters can be identified.

One of the authors, John Murray, would like to acknowledge the award of an S.R.C. Studentship for the period of this research. We are particularly grateful to Dr R. N. Haward and Dr J. Mann of Carrington Plastics Laboratory, Shell Chemical Co. Ltd, Urmston, Manchester and Dr E. Howells of Polymer and Petrochemical Laboratories, I.C.I. Ltd, Runcorn, for valuable discussion and assistance in the preparation of materials.

Department of Metallurgy and Materials Science,
The University of Liverpool.

(*Received August 1968*)

REFERENCES

[1]KAMBOUR, R. P. *J. Polym. Sci. A2*, 1966, **4**, 17
[2]MANN, J. Private communication
[3]KAMBOUR, R. P. *J. Polym. Sci. A2*, 1966, **4**, 349
[4]WOLOCK, I., KIES, J. A. and NEWMAN, S. B. in *Fracture*, p 250, B. L. AVERBACH, D. K. FELBECK, G. T. HAHN, and D. A. THOMAS, Eds. Wiley: New York, 1959
[5]KAMBOUR, R. P. *J. Polym. Sci. A*, 1964, **2**, 4159
[6]BIRD, R. J., MANN, J., POGANY, G. and ROONEY, G. *Polymer, Lond.* 1966, **7**, 307
[7]WOLOCK, I. and NEWMAN, S. B. in *Fracture Processes in Polymeric Solids*, p 240. B. ROSEN, Ed. Wiley: New York, 1964
[8]BERRY, J. P. *J. appl. Phys.* 1962, **33**, 1741
[9]BERRY, J. P. *J. Polym. Sci.* 1961, **50**, 313
[10]KAMBOUR, R. P. and BARKER, R. E. *J. Polym. Sci. A2*, 1966, **4**, 359
[11]YOFFE, E. H. *Phil. Mag.* 1951, **42**, 739